Available online at www.sciencedirect.com
SCIENCE DIRECT®
Carbon 43 (2005) 1743–1748
CARBON
www.elsevier.com/locate/carbon

# Iron particles in carbon nanotubes

Hansoo Kim [a,*], Wolfgang Sigmund [b]

[a] Department of Materials Science and Engineering, University of Pennsylvania, Philadelphia, PA 19104, USA
[b] Department of Materials Science and Engineering, University of Florida, Gainesville, FL 32611, USA

Received 11 September 2004; accepted 12 February 2005
Available online 21 March 2005

**Abstract**

Nanometer-size iron-rich particles in carbon nanotubes have been studied by transmission electron microscopy with and without in situ and ex situ heating. Several remarkable results were found; a high temperature phase (γ-Fe) of iron stable at low temperatures and preferential presence of iron and iron carbide in carbon nanotubes. Based upon these experimental results, thermodynamics of the Fe–C phase diagram and its kinetics were used to explain the non-uniform distribution of iron and iron carbide, which also yielded a deeper insight into the formation of carbon nanotubes. Some of the results also allowed describing the role of the graphitic structure in retaining the high temperature phase (γ-Fe) of iron at low temperatures. Furthermore, methods have been demonstrated with which γ-Fe can be produced in carbon nanotubes intentionally or in a large quantity. Selected area electron diffraction patterns of iron inside nanotubes demonstrated the crystallographic relationship of the iron to the nanotube axis along with phase changes of the iron. This paper summarizes the findings and draws further conclusions on the particle shape inside multiwalled carbon nanotubes.


*Keywords:* Carbon nanotubes; Transmission electron microscopy; Crystal structure

## 1. Introduction

Carbon nanotubes (CNTs) are crystalline graphitic sheets rolled up into a seamless cylindrical shape. Since their discovery diverse and unique physical properties of CNTs have been revealed. Therefore, many novel applications such as nanotube-based electronic circuits and field emission display [1,2] have been devised. CNTs can be produced through various methods using metallic particles as catalysts [3–5]. These catalytically grown CNTs may have residual catalyst particles inside and outside the nanotubes. The residual particles are normally removed before further processing [6–8] since they affect the original properties of CNTs. On the other hand, materials inside the cavities of CNTs can behave abnormally to show a subtle diversity in their phase diagram or novel physical properties as a consequence of increases in the surface-to-volume ratio, incomplete bonds, and the relative interaction between the materials and the inner walls of the nanotubes [9–11]. Therefore, it is important to observe the morphology and phase of residual catalyst particles for a better understanding of the growth mechanism for CNTs and the properties of the residual-catalyst containing CNTs.

While progress has been made in their applications, the growth mechanism of CNTs is not clearly understood. Various mechanisms have been suggested up to now based on the VLS (vapor–liquid–solid) theory [12–15] but a clear insight into thermodynamics during synthesis has not been available. For example, the physical state and chemical composition of catalyst particles during synthesis of CNTs are not known. According

* Corresponding author. Tel.: +1 215 573 1179; fax: +1 215 573 2128.
*E-mail address:* hansoo@seas.upenn.edu (H. Kim).

0008-6223/$ - see front matter © 2005 Elsevier Ltd. All rights reserved.
doi:10.1016/j.carbon.2005.02.019

to the previous mechanisms, carbon from a carbon source such as methane or xylene is dissolved into catalyst particles in the liquid (molten) state and reprecipitated as nanotubes. However, CNTs can be produced even far below the carbon-catalyst eutectic temperature [16,17]. Also, it is not clear whether the metallic particles catalyze the synthetic reactions in the form of a pure element or a metallic carbide. Therefore, a detailed investigation into residual catalyst particles in CNTs may open ways of optimizing the catalytic process and utilizing these particles, affording a clear insight into thermodynamics for the growth of CNTs.

Iron is one of the most frequently-used catalysts for the preparation of CNTs. Iron has a body-centered cubic (BCC) crystal structure (α-Fe, space group: Im3m) in the ambient atmosphere. α-Fe transforms to γ-Fe (space group: Fm3m) with a face-centered cubic (FCC) crystal structure at 912 °C. At 1394 °C γ-Fe transforms back to the BCC structure (δ-Fe) before it melts at 1538 °C [18]. Iron-rich particles encapsulated as a residue inside the cavities of CNTs or in a graphitic film have been probed thoroughly by transmission electron microscopy (TEM) to find out their crystallographic structures and orientations under various conditions and to understand the growth mechanism of CNTs [19–22]. In this paper these previous experiments and their results are reviewed.

## 2. Experiment

The materials used in these studies were multiwalled carbon nanotubes (MWNTs) synthesized at 700 °C by chemical vapor deposition. As mentioned above, at this temperature α-Fe is the stable phase of iron. Ferrocene ($Fe(C_5H_5)_2$) and xylene ($C_6H_4(CH_3)_2$) were used as sources for the catalyst and carbon, respectively. These CNTs contained nanometer-size iron-rich particles (normally of a rod shape) inside their cavities [19]. For these particles, high resolution, bright and dark field TEM images, selected area electron diffraction (SAED) patterns, and fast Fourier transforms were taken and analyzed. To test the effect of a graphitic structure on the iron phase diagram, submicrometer-size iron particles were placed on an amorphous carbon film and irradiated with the electron beam in situ inside the TEM [20]. Also, the residual iron particles in CNTs were irradiated by the electron beam in situ inside the TEM [21] or annealed ex situ by a heating element [22] and monitored for changes in morphology and phase of the particles.

## 3. Results and discussion

Through the analyses, a high temperature phase of iron (γ-Fe) was found to be stable in a large quantity (~40% of total iron particles) inside the cavities of CNTs even though the nanotubes were synthesized below the α-to-γ transition temperature [19,22]. Fig. 1 shows a typical γ-Fe particle in an as-synthesized MWNT. The other particles inside the cavities of CNTs were the stable α-Fe and a small fraction of iron carbide ($Fe_3C$). In contrast, at the tips of CNTs iron carbide was observed to be dominant with a smaller number of α-Fe

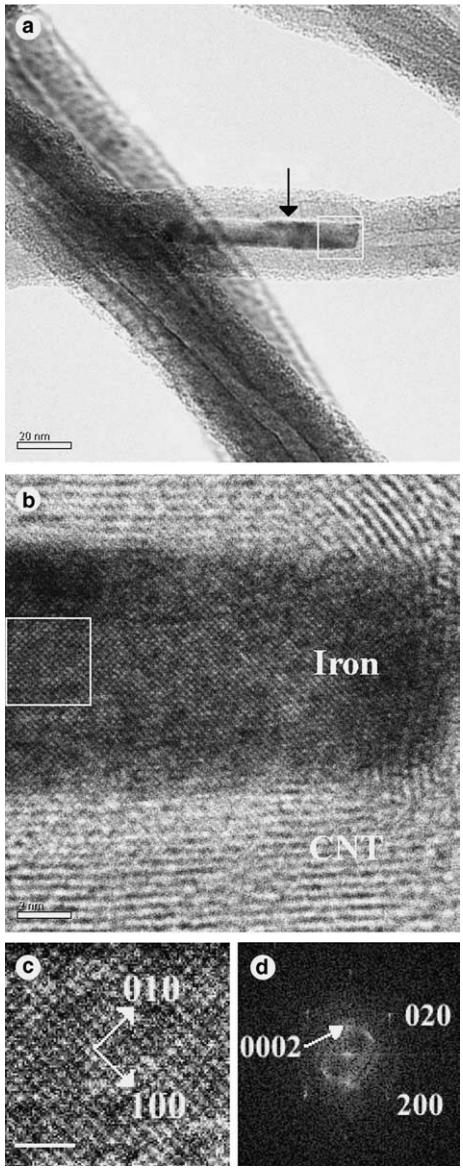


Fig. 1. A typical nanometer-size γ-Fe particle in a CNT. (a) A bright field (BF) TEM image of a high temperature phase (γ-Fe) of iron (pointed at by the arrow) in a CNT (scale bar: 20 nm). (b) A high resolution (HR) TEM image magnified from the white box in (a) showing the wall fringes of the CNT and the lattice fringes of the iron (scale bar: 2 nm). (c) A HRTEM image magnified further from the white box in (b) showing the lattice fringes of the γ-Fe aligned along the 001 zone (scale bar: 1 nm). (d) Fast Fourier transform of the high resolution TEM image in (b) shows spots corresponding to the (0002) planes of a CNT, and the (200) and (020) planes of γ-Fe.

particles. (In these papers [19–22] 'the cavity of a CNT' indicates the space enclosed by the innermost wall of the nanotube, excluding both tips.) Most of these iron-rich particles were found to be single crystals. Since the synthetic temperature (700 °C) is close to the stable (738 °C) and metastable (727 °C) eutectoid temperatures in the iron–carbon system, where γ-Fe, α-Fe, and carbon (or $Fe_3C$) may coexist [18], the formation of either γ-Fe or α-Fe is expected to have similar energetics during the growth of CNTs. Some γ-Fe particles formed during synthesis may have a tight contact with the inner walls of CNTs. Since the volume of γ-Fe needs to be increased by about 9% to transform to α-Fe, these γ-Fe particles in a tight contact with CNTs can retain their crystal structure even at room temperature due to the high elastic modulus (~1 TPa) of CNTs [23]. This may explain why the high temperature phase of iron (γ-Fe) is observed at room temperature inside the cavities of CNTs synthesized below the α–γ transition temperature. The fact that most $Fe_3C$ particles are at the tips while most iron particles are inside the cavities of CNTs may be a crucial key to understanding the growth mechanism of the nanotubes. It is well known that $Fe_3C$ forms a metastable equilibrium with both γ-Fe and α-Fe while graphite forms a stable equilibrium with these iron phases. However, there is no stable or metastable equilibrium between $Fe_3C$ and graphite (this is why we cannot see phase regions above 6.7 wt.% carbon in the iron–carbon phase diagram). When $Fe_3C$ and graphite are in contact, $Fe_3C$ easily decomposes to iron and carbon especially at high temperatures. Therefore, when $Fe_3C$ is at the growing tip of a CNT during synthesis, its part contacting with the nanotube should be decomposed into iron and carbon. The iron may form a layer between the $Fe_3C$ and the nanotube to make a stable equilibrium with the nanotube and a metastable equilibrium with the $Fe_3C$ while the carbon may participate in forming the graphitic structure of the nanotube. This iron layer can be pinched off during further growth of CNTs to form iron particles inside the cavities, holding $Fe_3C$ at the tips. Fig. 2 shows the growing tip in this model and a real tip of a CNT for comparison. A so-called 'metal dusting' process supports this hypothesis [24–26]. According to this process, when bulk iron is exposed to a large amount of carbon in the temperature range of 400–800 °C, $Fe_3C$ and graphite are produced on its surface and a thin layer of iron is formed later between the $Fe_3C$ and the graphite as a result of the decomposition of $Fe_3C$. This iron layer acts as a catalyst for further deposition of carbon. Therefore, this may explain the non-uniform distribution of iron and iron carbide in CNTs (in the cavities and at the tips) and give a clue to the growth mechanism of the nanotubes.

Another important feature found with the MWNTs is that they contain rod-shape iron particles even though they were produced far below the melting temperature

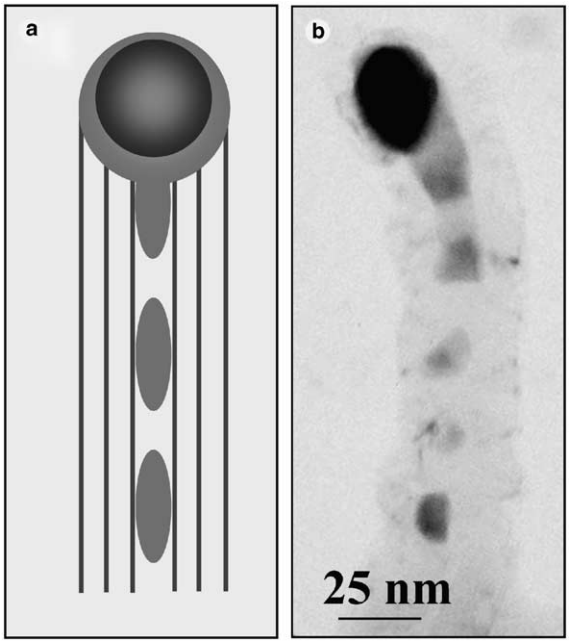


Fig. 2. Comparison of the tip of a CNT in the suggested mechanism with a real tip. (a) A schematic of the mechanism suggested for the growth of a CNT where the black lines, the dark gray sphere, and the other gray parts stand for walls of a CNT, iron carbide, and iron, respectively. The iron layer between iron carbide and a growing CNT may be pinched off and form discontinuous iron particles in the cavity. (b) A BF TEM image of a real tip of a CNT containing iron-rich particles. Note the similarities between the schematic and the BF TEM image.

of iron. In the suggested mechanisms [12–14] the catalyst particles should be in the liquid state as mentioned above, molding themselves into a rod to the shape of the cavities of CNTs. Therefore, the rod-shaped iron-rich particles appear to support the mechanisms. However, it is hard to believe that at the synthetic temperature (700 °C) the catalyst particles with a diameter of larger than 5 nm were in the liquid state, even considering the exothermal decomposition of the carbon source and a high carbon concentration. This apparent discrepancy may be explained by the abnormal behavior of small metallic particles on a substrate. It is known that even far below the melting temperature, particles of small sizes (sub-micrometer to a few micrometer in diameter) on a substrate can behave like they are in the liquid state [27–30]. In the reports Ag islands evaporated onto NaCl coalesce like liquid even at 100 °C (melting temperature of Ag is 961 °C), and Ag crystallites on graphite or an amorphous carbon film move randomly like liquid droplets also below the melting temperature even though diffraction patterns or Moiré patterns show the Ag islands and crystallites are in the solid state. Therefore, the iron particles in CNTs are expected to take a rod shape even in the solid state during synthesis as a result of the liquid-like property of the particles on the inner walls of the nanotubes.

To evaluate the role of the high elastic modulus of a graphitic structure in stabilizing γ-Fe, it was investigated whether γ-Fe could be stable without a graphitic structure such as CNTs and graphitic films. To do this, oxidized submicrometer-size iron particles on an amorphous carbon film were irradiated by the electron beam in situ inside TEM [20]. It was found that by the electron irradiation the oxidized iron particles could be reduced to α-Fe, γ-Fe, and $Fe_3C$, often forming a graphitic film on the surface through interaction with the underlying amorphous carbon during the reduction process. Fig. 3 shows an example in which an oxidized iron particle was fractured and reduced by the electron beam to form an γ-Fe particle with a graphitic film on its surface. In this experiment, all γ-Fe particles were observed to be encapsulated in a graphitic film, indicating that a graphitic structure is indispensable for retaining γ-Fe at low temperatures. Namely, the high elastic modulus of graphite [31] can suppress the volume increase of γ-Fe necessary for its transformation into α-Fe even at room temperature. This result may open a way of controlling phase of iron in a CNT. In fact, it was found that when α-Fe in CNTs is irradiated by the electron beam in situ inside TEM it is transformed to a stable γ-Fe efficiently (~80%) without damaging the nanotubes [21]. Fig. 4 demonstrates one example. The long α-Fe particle encapsulated in a MWNT (Fig. 4(a) and (b)) transformed to γ-Fe (Fig. 4(c) and (d)) with a large reduction in aspect ratio after the beam irradiation. Furthermore, it was also found that when CNTs are annealed by a heating element in a furnace, the number ratio of γ-Fe to α-Fe particles in the nanotubes is greatly increased up to about 2 from 0.7 for iron in as-synthesized CNTs [22]. The formation of γ-Fe is accomplished by the heat transfer to α-Fe from the incident electrons or the heating element. The heat may raise the temperature of α-Fe above the α–γ transition temperature. The retention of γ-Fe in CNTs at room temperature is attributed to the formation of a tight contact between the γ-Fe and the nanotubes through an increase in diameter of the iron, and the high elastic modulus of CNTs. The increase in diameter of iron particles in CNTs may be caused by the decrease in their aspect ratios in the solid state or melting depending on experimental temperatures [21,22]. Carbon dissolved into iron particles may play an important role in lowering their melting temperature and stabilizing undercooled γ-Fe [22].

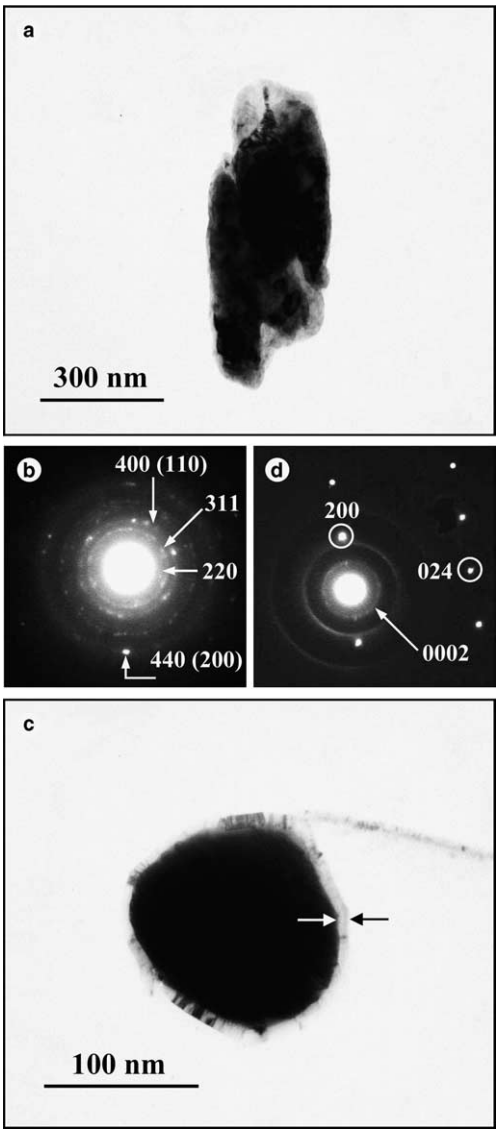


Fig. 3. Formation of γ-Fe encapsulated in a graphitic film by the electron beam. (a) A BF TEM image of an iron particle (the dark object) on an amorphous carbon film (background) before the beam irradiation. (b) An SAED pattern taken from the particle in (a) showing its polycrystalline crystal structure. Each diffraction ring is indexed as crystal planes of γ-$Fe_2O_3$ or α-Fe. Parenthesized indices correspond to the planes of α-Fe. (c) A BF TEM image of one of the particles formed from fracture of the particle in (a) by the electron beam. The arrows indicate a graphitic film on the surface of the particle. (d) An SAED pattern taken from the particle in (c) shows the $02\bar{1}$ zone of γ-Fe and the 0002 diffraction ring of a graphitic film. The other diffraction rings come from the carbon film.

It was also found that iron particles in CNTs are aligned in specific crystallographic orientations of each crystal structure [22]. Therefore, along the axis of CNTs α-Fe is oriented in the ⟨001⟩ or ⟨111⟩ directions of its BCC structure while γ-Fe is in the ⟨110⟩ directions of its FCC structure. These iron particles may be used to modify the electronic properties of CNTs like metallofullerenes in CNTs [32]. For example, α-Fe in a CNT can be transformed selectively to γ-Fe by the electron beam, which will differentiate three dissimilar parts of the nanotube (two parts containing γ-Fe or α-Fe, and the part containing no iron) due to the pressure applied by γ-Fe [33,34] and the charge transfer between iron and a CNT. γ-Fe has a tendency to transform back to α-Fe at room temperature, applying pressure on the wall of a CNT where it is encapsulated. Also, the charge transfer between γ-Fe (or α-Fe) and a CNT induced by

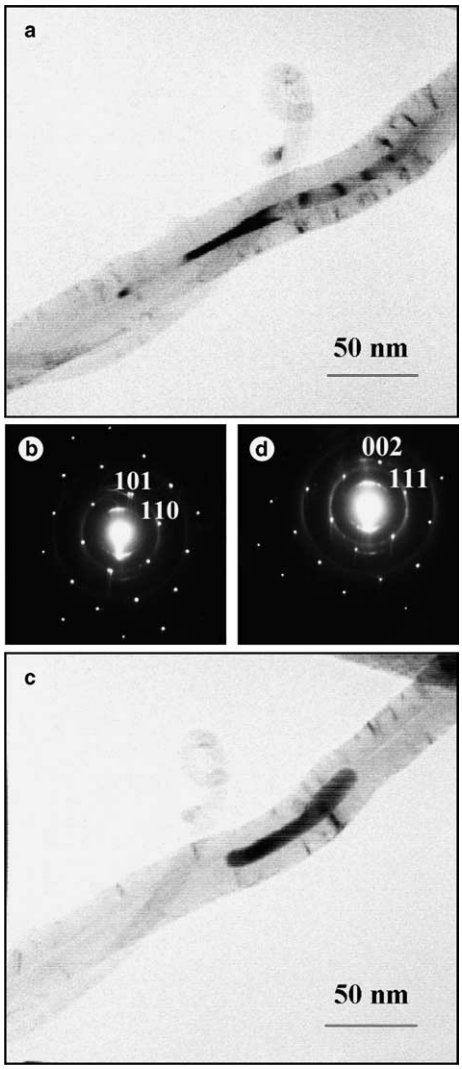


Fig. 4. Phase transformation of iron in a CNT by the electron irradiation. (a) A BF TEM image of a CNT containing a long iron particle. (b) An SAED pattern taken from the iron particle in (a) showing the $\bar{1}11$ zone of α-Fe. (c) A BF TEM image of the iron particle after the electron irradiation. (d) An SAED pattern taken from the iron particle in (a) showing the $\bar{1}10$ zone of γ-Fe.

the difference in their values of the work function will change the energy band structure of the nanotube.

## 4. Conclusions

In conclusion, nanometer-size iron-rich particles encapsulated in CNTs have been investigated under various conditions. It was found that inside the cavities of as-synthesized CNTs the high and low temperature phases (γ-Fe and α-Fe) of iron are dominant whereas most of the residual particles at their tips are iron carbide. From this fact, the mechanism for the non-uniform distribution of iron and iron carbide, and the formation of CNTs is suggested based upon the metal dusting process. Also, the reason that iron has normally a rod shape inside the cavities of CNTs is suggested by the liquid-like properties of small metal particles on a substrate. The in situ irradiation of small iron particles on an amorphous carbon showed that graphitic structures are necessary for retaining gamma-Fe at low temperatures. From this fact, methods have been devised, by which gamma-Fe can be produced intentionally inside the cavities of CNTs (by the electron beam or by a heating element). Analyses of SAED patterns taken from the iron particles inside the cavities of CNTs revealed that they are aligned along specific crystallographic directions of each crystal structure. These results from the detailed investigation into iron-rich particles in CNTs provide fundamental information on the catalytic mechanism. Furthermore, controlling the crystal structure of the encapsulated catalyst particles may lead to modifying the physical properties of their host CNT.

## References

[1] Tans SJ, Verschueren ARM, Dekker C. Room-temperature transistor based on a single carbon nanotube. Nature 1998;393:49–52.
[2] Normile D. Nanotubes generate full-color displays. Science 1999;286:2056–7.
[3] Loiseau A, Pascard H. Synthesis of long carbon nanotubes filled with Se, S, Sb and Ge by the arc method. Chem Phys Lett 1996;256:246–52.
[4] Zhang M, Yudasaka M, Iijima S. Single-wall carbon nanotubes: a high yield of tubes through laser ablation of a crude-tube target. Chem Phys Lett 2001;336:196–200.
[5] Kukovitsky EF, L'vov SG, Sainov NA, Shustov VA. CVD growth of carbon nanotube films on nickel substrates. Appl Surf Sci 2003;215:201–8.
[6] Chiang IW, Brinson BE, Huang AY, Willis PA, Bronikowski MJ, Margrave JL, et al. Purification and characterization of single-wall carbon nanotubes (SWNTs) obtained from the gas-phase decomposition of CO (HiPco Process). J Phys Chem B 2001;105:8297–301.
[7] Strong KL, Anderson DP, Lafdi K, Kuhn JN. Purification process for single-wall carbon nanotubes. Carbon 2003;41:1477–88.
[8] Harutyunyan AR, Pradhan BK, Chang JP, Chen GG, Eklund PC. Purification of single-wall carbon nanotubes by selective microwave heating of catalyst particles. J Phys Chem B 2002;106:8671–5.
[9] Koga K, Gao GT, Tanaka H, Zeng XC. Formation of ordered ice nanotubes inside carbon nanotubes. Nature 2001;412:802–5.
[10] Gao Y, Bando Y, Goldberg D. Melting and expansion behavior of indium in carbon nanotubes. Appl Phys Lett 2002;81:4133–5.
[11] Sloan J, Kirkland AI, Hutchson JL, Green MLH. Integral atomic layer architectures of 1D crystals inserted into single walled carbon nanotubes. Chem Comm 2002;13:1319–32.
[12] Kukovistsky EF, L'vov SG, Sainov NA. VLS-growth of carbon nanotubes from the vapor. Chem Phys Lett 2000;317:65–70.
[13] Kanzow H, Ding A. Formation mechanism of single-wall carbon nanotubes on liquid-metal particles. Phys Rev B 1999;60:11180–6.
[14] Gorbunov A, Jost O, Pompe W, Graff A. Solid–liquid–solid growth mechanism of single-wall carbon nanotubes. Carbon 2002;40:113–8.
[15] Wagner RS, Ellis WC. Vapor–liquid–solid mechanism of single crystal growth. Appl Phys Lett 1964;4:89–90.

[16] Dillon AC, Mahan AH, Alleman JL, Heben MJ, Parilla PA, Jones KM. Hot-wire chemical vapor deposition of carbon nanotubes. Thin Solid Films 2003;430:292–5.
[17] Benito AM, Maniette Y, Muñoz E, Martínez MT. Carbon nanotubes production by catalytic pyrolysis of benzene. Carbon 1998;36:681–3.
[18] Shackelford JF. Introduction to materials science for engineers. 2nd ed. New York: Macmillan; 1990. p. 215–20.
[19] Kim H, Kaufman MJ, Sigmund WM, Jacques D, Andrews R. Observation and formation mechanism of stable FCC Fe nanorods in carbon nanotubes. J Mater Res 2003;18:1104–8.
[20] Kim H, Sigmund WM. Effect of a graphitic structure on the stability of FCC iron. J Cryst Growth 2004;267:738–44.
[21] Kim H, Kaufman M, Sigmund WM. Phase transition of iron inside carbon nanotubes under electron irradiation. J Mater Res 2004;19:1835–9.
[22] Kim H, Sigmund WM. Iron nanoparticles inside carbon nanotubes at various temperatures. J Cryst Grow 2005;276:603–14.
[23] Wong EW, Sheehan PE, Lieber CM. Nanobeam mechanics: elasticity, strength, and toughness of nanorods and nanotubes. Science 1997;277:1971–5.
[24] Hochman RF. Catastrophic deterioration of high temperature alloys in carbonaceous atmospheres. In: Proc. of the Symp. on Properties of high temperature alloys with emphasis on environmental effects. Electrochem Soc Inc Proc 1976;77:715–32.
[25] Grabke HJ. Thermodynamics, mechanisms and kinetics of metal dusting. Mater Corros 1998;49:303–8.
[26] Schneider A. Iron layer formation during cementite decomposition in carburizing atmospheres. Corros Sci 2002;44:2353–65.
[27] Chopra KL. Thin film phenomena. New York: MacGraw-Hill; 1969. p. 166–71.
[28] Bassett GA. Proc Eur Regional Conf Electron Microscopy Delft 1960 1961;1:270–5.
[29] Sears GW, Hudson JB. Mobility of silver crystallites on surfaces of $MoS_2$ and graphite. J Chem Phys 1963;39:2380–1.
[30] Thomas JM, Walker PL. Mobility of metal particles on a graphite substrate. J Chem Phys 1964;41:587–8.
[31] Blakeslee OL, Proctor DG, Seldin EJ, Spence GB, Weng T. Elastic constants of compression-annealed pyrolytic graphite. J Appl Phys 1970;41:3373–82.
[32] Lee J, Kim H, Kahng SJ, Kim G, Son YW, Ihm J, et al. Bandgap modulation of carbon nanotubes by encapsulated metallofullerenes. Nature 2002;415:1005–8.
[33] Heyd R, Charlier A, McRae E. Uniaxial-stress effects on the electronic properties of carbon nanotubes. Phys Rev B 1997;55:6820–4.
[34] Yang L, Anantram MP, Han J, Lu JP. Band-gap change of carbon nanotubes: effect of small uniaxial and torsional strain. Phys Rev B 1999;60:13874–8.